

# SUSY searches in the single lepton channel in the High Luminosity LHC

Sergio Sánchez Cruz

Supervisors: Isabell Melzer-Pellmann

Claudia Seitz

September 8, 2014

## Abstract

In this project, a search for Supersymmetry in pp collisions at the LHC is performed. The analysis studies collisions at a center-of-mass energy  $\sqrt{s} = 14$  TeVup, emulating the conditions of the High Luminosity-LHC. Three benchmark scenarios based on supersymmetric models are chosen to estimate the discovery sensitivity of an upgraded detector with 300 and 3000  $fb^{-1}$  of data.

# Contents

<b>1. Theoretical justification of SUSY</b>	<b>3</b>
1.1. The Standard Model and its limitations . . . . .	3
1.2. Supersymmetry . . . . .	4
1.3. Other features of SUSY . . . . .	5
<b>2. Experimental searches of SUSY</b>	<b>6</b>
<b>3. The Large Hadron Collider</b>	<b>6</b>
3.1. Detectors at LHC . . . . .	6
3.2. CMS . . . . .	6
3.2.1. Reconstruction of particles . . . . .	7
3.3. High Luminosity LHC . . . . .	8
<b>4. Discussion of the full models</b>	<b>9</b>
4.1. Data samples . . . . .	9
4.1.1. Fast simulation: DELPHES . . . . .	9
<b>5. Event selection</b>	<b>10</b>
5.1. Object selection . . . . .	11
5.1.1. Multiplicities . . . . .	11
5.2. Preselection . . . . .	11
5.3. Cuts on $H_T$ and MET . . . . .	11
<b>6. Expected discovery sensitivity</b>	<b>14</b>
6.1. Methods . . . . .	14
6.2. Shape analysis . . . . .	16
<b>7. Conclusion</b>	<b>17</b>
<b>8. Acknowledgments</b>	<b>18</b>
<b>A. Cut flow</b>	<b>19</b>
<b>Acronyms</b>	<b>21</b>
<b>References</b>	<b>22</b>

# 1. Theoretical justification of SUSY

## 1.1. The Standard Model and its limitations

The standard model (SM) of particle physics provides a description for most of the observed phenomena in modern high energy physics. It includes a self-consistent characterization of all the particles that constitute matter and participate in its interactions. The SM is thought to be one of the most exact theories in the history of science, and the discovery of the Higgs boson at the LHC in 2012 has proven its phenomenological success.

Gravitational interactions are not included in the SM, since it there is so far no appropriate renormalizable field theory describing this phenomena. For this and other reasons, it is believed that the SM is an effective low-energy theory, rather than a complete description of nature.

We quote some of the problems for which the SM does not provide an answer:

- As previously mentioned, the SM does not provide a convenient description of gravity.
- Empirical observations of the galaxy rotation curves are not consistent with the amount of visible matter in the galaxies. Cosmologists have therefore predicted the existence of a yet unknown kind of matter, called dark matter.

Dark matter is thought to be very massive, weakly interacting, electrically neutral and without color charge. It is also supposed to be cold. The only massive neutral and colorless particle included in the SM is the neutrino, which is known to be light and, therefore, hot. Thus, SM does not provide any suitable candidate for dark matter.

- Observations of the Cosmic Microwave Background (CMB) suggests an expansion of the universe. This suggestion is somewhat confirmed by the observation of a big redshift of the light from remote galaxies. A possible explanation for this expansion is the so-called dark energy. The SM does not provide any particle or field that would constitute dark matter.
- Models that explain the evolution of the universe in its earlier stages predict that the amount of matter and antimatter in the universe should be the equal in absence of CP violation sources. The maximal CP violation allowed in the SM predicts a ratio of matter to antimatter of  $10^{-10}$ . This ratio is observed to be  $10^{-20}$ . Thus, the theory should be corrected in order to allow additional sources of CP violation.
- Neutrinos in the SM are expected to be massless. Yet, the neutrinos are known to be massive, due to experimental results that show neutrino oscillations.
- In the search for a complete description of nature, it is philosophically desirable to find a Grand Unified Theory (GUT) which unifies the three forces described by the SM at the Planck scale. Including gravity as the fourth force would provide a

theory of everything (TOE). Since in the SM the strong, weak and electromagnetic coupling constants are not equal at the Planck scale, it fails to be a GUT.

- The hierarchy problem arises when trying to compute the fermion loop corrections to the mass of a scalar particle, namely the Higgs boson. The corrections to the masses are proportional to the expression [1]:

$$m_H^2 = m_{H_0}^2 - \frac{|\lambda_f|^2}{8\pi^2} \Lambda^2, \quad (1)$$

where  $\Lambda$  is a cut-off scale, which is interpreted as the maximum energy scale at which the theory is valid and which is, at least, the order of the Planck scale,  $1.22 \cdot 10^{19}$  GeV. The correction is proportional to  $\Lambda^2$ , which means that the corrections are of the order of  $10^{30} M_H$ . The discovery of a low-mass Higgs boson suggests that additional Feynman diagrams should be taken into account.

## 1.2. Supersymmetry

One of the main goals of fundamental physics is to find an extension of SM which provides a solutions to the problems. Supersymmetry (SUSY) is one of the main candidates to fulfil this purpose. It can be justified as a natural solution to the hierarchy problem. Moreover, it also provides feasible solutions or explanations for some of the unknowns stated in the previous section.

SUSY establishes that, since bosons can compensate the divergence of the Higgs mass due to the fermions, the correction would be zero if there was a symmetry in nature which assigns an equal mass fermion to every boson and a equal mass boson to every fermion, so that every fermionic loop would be annihilated by a bosonic loop and viceversa. The symmetry can be written:

$$\begin{aligned} Q |fermion\rangle &= |boson\rangle \\ Q |boson\rangle &= |fermion\rangle \end{aligned}$$

This postulates the existence of new particles, called supersymmetric particles or *sparticles*. Each SM particle as assigned a SUSY particle which we will refer to as its SUSY partner. SUSY partners of leptons are called *sleptons* (and, thus, the SUSY partner of the electron will be the selectron) and the SUSY partners of bosons are called *gaugino*. The complete list of SUSY particles is summarized in table 1 [2]. The theory also introduces a new quantum number, R-parity, defined as  $P_R = (-1)^{2S+3B+L}$ , where  $S$  is the spin,  $B$  the baryon number and  $L$  the lepton number. R-parity is +1 for SM particles and -1 for SUSY particles. The conservation of this number implies that SUSY particles are produced in pairs and decay to a stable SUSY particle, called Lightest SuperSymmetric Particle (LSP). The LSP is stable, neutral and colorless.

However, experimental results show that such a symmetry does not hold: if it was true, SUSY particles would have already been observed. A scenario in which SUSY is broken may also provide a solution for the hierarchy problem. The mass of the SUSY particle can be written as

$$m_{\tilde{f}}^2 = m_f^2 + \Delta^2 \quad (2)$$

Names	Spin	$P_R$	Gauge Eigenstates	Mass Eigenstates
Higgs bosons	0	+1	$H_u^0 H_d^0 H_u^+ H_d^-$	$h^0 H^0 A^0 H^\pm$
squarks	0	-1	$\tilde{u}_L \tilde{u}_R \tilde{d}_L \tilde{d}_R$	(same)
			$\tilde{s}_L \tilde{s}_R \tilde{c}_L \tilde{c}_R$	(same)
			$\tilde{t}_L \tilde{t}_R \tilde{b}_L \tilde{b}_R$	$\tilde{t}_1 \tilde{t}_2 \tilde{b}_1 \tilde{b}_2$
sleptons	0	-1	$\tilde{e}_L \tilde{e}_R \tilde{\nu}_e$	(same)
			$\tilde{\mu}_L \tilde{\mu}_R \tilde{\nu}_\mu$	(same)
			$\tilde{\tau}_L \tilde{\tau}_R \tilde{\nu}_\tau$	$\tilde{\tau}_1 \tilde{\tau}_2 \tilde{\nu}_\tau$
neutralinos	1/2	-1	$\tilde{B}^0 \tilde{W}^0 \tilde{H}_u^0 \tilde{H}_d^0$	$\tilde{N}_1 \tilde{N}_2 \tilde{N}_3 \tilde{N}_4$
charginos	1/2	-1	$\tilde{W}^\pm \tilde{H}_u^\pm \tilde{H}_d^\pm$	$\tilde{C}_1^\pm \tilde{C}_2^\pm$
gluinos	1/2	-1	$\tilde{g}$	(same)
goldstino (gravitino)	1/2 (3/2)	-1	$\tilde{G}$	(same)

**Table 1:** List of all the SUSY particles: mass and gauge eigenstates.

Then the correction to the Higgs mass due to the loops is proportional to  $\Delta^2$ . This correction is sufficiently small when  $\Delta = \mathcal{O}(1 \text{ TeV})$ . This energy scale should be within the range of discovery of the LHC.

The symmetry breaking can be mediated by several terms in the Lagrangian of the model. The mass spectrum of the sparticles depends on the specific way the breaking is mediated. This leads to a great variety of models. The Minimal Supersymmetric Standard Model (MSSM) is the simplest extension of the SM to a SUSY theory. Despite of being minimal, it introduces 110 additional free parameters [3].

The experimental search for such a theory is extremely complex and constrained models are used. The constrained MSSM (cMSSM) reduces the number of free parameters to 5 plus one sign.

Other models are developed based on assumptions about the way the symmetry breaking is achieved.

### 1.3. Other features of SUSY

As previously mentioned, SUSY also provides answers to additional theoretical questions. Among others:

- Including SUSY terms into the SM Lagrangian leads to the unification of the strong, weak and electromagnetic forces at the Planck Scale.
- The LSP is known to be massive compared to SM particles. Moreover it is stable, neutral and colorless and therefore, it is an excellent candidate for dark matter.

- Additional SUSY terms in the Lagrangian allow additional sources of CP-violation. This could provide an explanation for the observed matter-antimatter asymmetry.

## 2. Experimental searches of SUSY

Despite of the efforts of the scientific community, sparticles have not been directly observed in any experiment. One of the main drawbacks for experiments is the variety of ways the symmetry can be broken, which leads to a number of simplified models with a few free parameters. Searches for these models only probe small regions of the full SUSY phase space.

## 3. The Large Hadron Collider

One of the most ambitious projects of experimental particle physics is the Large Hadron Collider (LHC), located at CERN, Switzerland.

LHC is a superconducting proton-proton collider with a circumference of 27 km. It was first used in 2010, colliding protons with a center-of-mass energy of  $\sqrt{s} = 7$  TeV and delivering a total integrated luminosity of  $47pb^{-1}$  to the experiments CMS and ATLAS. After 2011, the luminosity was raised, delivering  $5.7fb^{-1}$  of data. Between April 2012 and December 2012, the center of mass energy was raised up to 8 TeV. The total luminosity delivered to CMS and ATLAS in this first run was  $30fb^{-1}$ . Among the greatest achievements of this period is the discovery of the SM Higgs boson.

The LHC is currently in a shutdown until 2015, when it is expected that protons will collide with a higher  $\sqrt{s}$ , up to 14 TeV, the highest energy achieved in a collider.

### 3.1. Detectors at LHC

Protons are accelerated at the LHC ring and they collide in 4 spots, where the 4 experiments of LHC are located. Those experiments are ALICE, LHCb, ATLAS and CMS. A Large Ion Collider Experiment [4] (ALICE) is a heavy ion detector designed for the study of strong interactions in extreme density conditions. The Large Hadron Collider [5] (LHCb) beauty experiment is dedicated to the study of B-mesons in order to study flavour physics, specially CP violation. A Toroidal LHC Apparatus [6] (ATLAS) is a general purpose experiment, designed for a wide variety of physics measurements.

### 3.2. CMS

The Compact Muon Solenoid (CMS) is a general purpose detector. As the name implies, a lot of effort has been put in the detection of muons at a wide range of energy scales. We quote the main features of the detector in this section. A complete description can be found in [7].

The CMS detector is composed of three main parts, displayed schematically in figure 1: the tracking system, the calorimeters and the muon system. A solenoid magnet generates

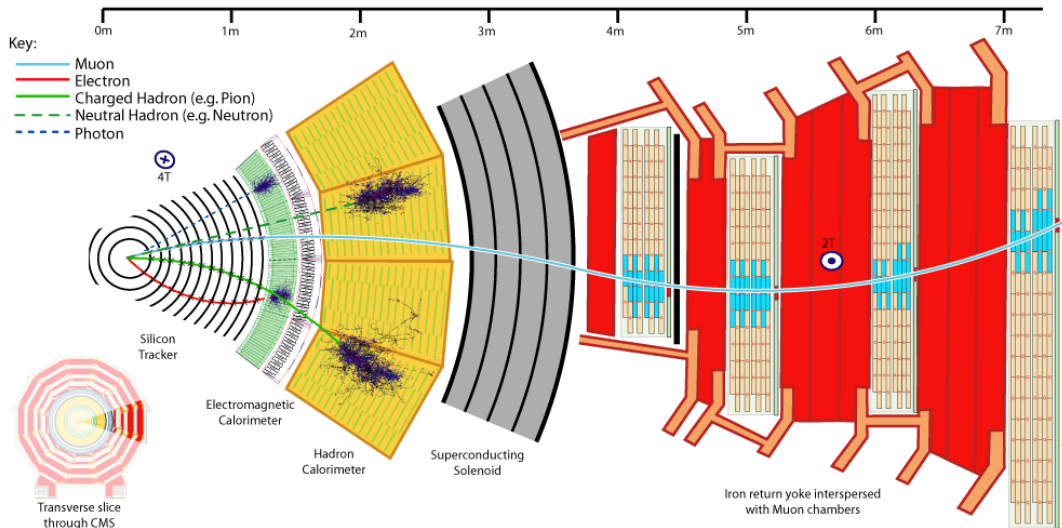


**Figure 1:** Schematical view of the CMS detector. The interaction of each type of particle with the detector is also shown.

a 4 T magnetic field along the beam axis. The magnetic field curves the charged particles in the transverse plane

The tracking system measures the trajectory of the charged particles produced in the collision. The curvature of the trajectory is related to the transverse momentum of the particle, via the relation  $R(m) = p_T(\text{GeV})/0.3B(\text{T})$ , where  $R$  the radius of curvature and  $B$  the magnetic field. The sign of the charge can also be determined by studying the direction of the curve.

The calorimeter measures the energy and direction of particles, allowing to reconstruct the type of particle produced in the collision. It is composed of two parts: the Electromagnetic Calorimeter (ECAL) and the Hadronic Calorimeter (HCAL). The ECAL detects light charged particles and photons, while the HCAL detects heavier charged and neutral particles.

Muons are weakly interacting particles, which pass through the calorimeters without leaving large amounts of energy. Therefore the outer part of the detector is comprised of the muon systems.

### 3.2.1. Reconstruction of particles

Each type of particle produced in collisions interacts differently with each layer of the detector, according to their fundamental properties.

- **Leptons.** The trajectory of electrons and muons is measured in the tracking system. Electrons produce showers in the ECAL, where their energy can be measured. Muons do not deposit all their energy in the inner detectors and can be measured in the muon system. The lower half-life of taus leads to a small flight distance

of the particle. Therefore, taus cannot be detected directly. However, its decay products can be measured.

- **Photons** are not detected in the tracking system and their trajectory is not curved by the magnetic field. Their energy is deposited in the ECAL.
- **Charged hadrons**, such as protons or  $\pi^\pm$ , are measured in the tracking system. They fly through the ECAL and deposit their energy in the HCAL.
- **Neutral hadrons** do not interact with the tracking system and deposit their energy in the HCAL.
- **Neutrinos** only interact via the weak force, therefore they do not interact with the detector. The presence of the neutrino in the final state of a collision can be inferred using the Missing Transverse Energy (MET), defined as

$$MET = \left| \sum_{\text{particles}} \vec{p}_T \right| \quad (3)$$

which is zero if all the particles are correctly detected and measured. A nonzero MET can also arise when measuring a collision with a LSP in the final state or due to mismeasurement of known particles.

- **Jets.** Due to the QCD confinement, color charged particles cannot exist free. However, these particles can be released in high-energy p-p collisions, fragmenting into hadronic showers before being detected. This showers are called jets, and can be reconstructed using several algorithms.

Jets produced by a b quark can be identified due to the presence of B-mesons in the jet. These mesons decay and produce secondary vertices that can be measured via a high precision tracking system. This process is called b-tagging. Several algorithms have been developed in order to perform the b-tagging efficiently and with a low misidentification rate [8].

### 3.3. High Luminosity LHC

During the runs II and III, the LHC will record a total amount of 300-350  $fb^{-1}$  of data. After that period, an upgrade needs to be performed in order to increase its discovery potential. This upgrade includes an improvement in the semiconducting magnets which will lead to a increase in the delivered luminosity. The total expected integrated luminosity is around 3000  $fb^{-1}$ , ten times higher than the luminosity for which it was built.

However, the increment in the instantaneous luminosity will produce an increment on additional interactions in the same event, called pile-up. This is estimated via the average number of reconstructed vertices in each bunch crossing. This number is expected to be 50 during runs II and III, while it will be 140 in the HL-LHC. This will lead to

lower resolution in some measured quantities. This project studies and compares both scenarios.

## 4. Discussion of the full models

In the present report, three natural pMSSM models are studied. These models contain production and decay channels which might be observed in the LHC pp collisions after a luminosity of either  $300 \text{ fb}^{-1}$  or  $3000 \text{ fb}^{-1}$  has been collected. The three models are motivated by cosmological constraints and differ by the composition of the LSP,  $\tilde{\chi}_1^0$ . The gluino has a discoverable mass of 1.7 TeV [10]. This analysis focuses on the  $\tilde{g}\tilde{g}$  pair production. In table 2b  $\tilde{g}$  branching ratios are shown. In table 2a, we quote the cross-section of each model, calculated next-to-leading order.

Model	$\sigma$ (pb)	Process	Branching ratio		
			NM1	NM2	NM3
NM1	0.10				
NM2	0.07	$\tilde{g} \rightarrow \tilde{t}_1 t$	60%	60%	60%
NM3	1.96	$\tilde{g} \rightarrow \tilde{b}_1 b$	40%	40%	40%

(a) Cross sections of the model calculated NLO. (b) Branching ratios of the  $\tilde{g}$  in each model.

**Table 2:** Relevant parameters of the studied models.

The top squark decays to top and  $\chi_1^0$  or  $\chi_2^0$ , while the bottom squark mainly decays to top quark and  $\chi_1^\pm$ , which decays to  $\chi_1^0$  and soft jets or a soft lepton and neutrino.

### 4.1. Data samples

The signal and background events are simulated using Monte Carlo methods (MC). The target signatures for this analysis includes one lepton in the final state, large MET, high jet and b-jet multiplicity and large  $H_T$ .

The background sources are  $t\bar{t}$  events, in which a lepton can produced in the decay of the W boson, single top events, V+jets and VV. V+jets and VV do not produce so many b-tagged jets, therefore their contribution is lower. The main background contribution comes from  $t\bar{t}$  events, whose signature is similar to the signal.

The signal events are calculated using SUSPECT 2.41/2.43 or SOFTSUSY 3.4.0 in combination with SUSY-HIT 1.3B/3.4. The resulting files are processed with MADEVENT, and hadronized with PYTHIA 6.4. The response of the detector is emulated with the DELPHES 3.0.10 detector simulation package.

#### 4.1.1. Fast simulation: Delphes

Due to the high luminosity, the number of simulated events is too high to perform a full simulation of the detector on all of them. The fast simulation software DELPHES [12] is

used instead.

Fast simulation does not require extensive computational resources and is 2-3 orders of magnitude faster than full simulation. The precision provided by fast simulation software is suitable for most phenomenological studies. Instead of simulating the whole detector, Delphes computes the energy of the outgoing particles smearing the initial momenta according to the resolution of the detector. However, the newer versions of Delphes emulate the particle-flow reconstruction philosophy by simulating every sub-detector separately.

## 5. Event selection

The events are selected focusing on the  $\tilde{g}\tilde{g}$  production, following the simplified model shown in figure 2. The selection criteria are chosen using  $\tilde{g}\tilde{g}$  events, selected from the sample using MC truth.

The topology of the final state includes up to 4 leptons, products of the top quark decay. We will restrict to the one lepton channel. The expected signature of the signal includes large MET, due to the presence of two  $\tilde{\chi}_1^0$ , which do not interact with the detector, and a large hadronic activity. The hadronic activity can be estimated via the jet multiplicity or via the magnitude  $H_T$ , defined by

$$H_T = \sum_{jets} |p_T| \quad (4)$$

where the sum is performed over all selected jets.

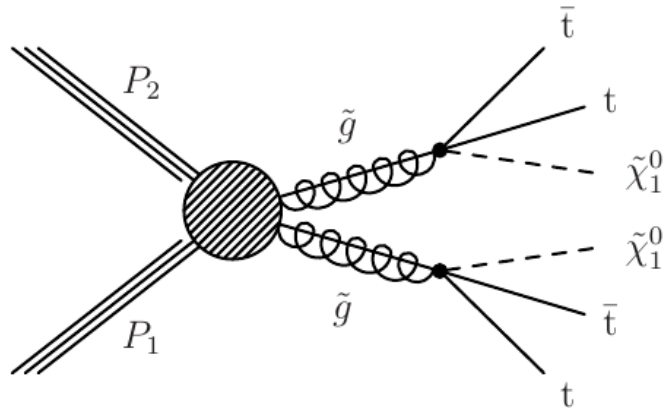


**Figure 2:** Simplified model of the expected decay of  $\tilde{g}\tilde{g}$

Additionally, since the top quark decays into a W boson and a b-quark with a probability close to 1, up to 4 b-tagged jets are expected in signal events.

## 5.1. Object selection

Objects are selected based on the expected signal event topology. Electron candidates were required to have a  $p_T$  greater than 10 GeV and  $|\eta| < 2.4$ , while muon candidates were required to have  $p_T > 10$  GeV and  $|\eta| < 2.1$ . Additionally, the lepton candidates are expected to be isolated. We define the isolation of a lepton as

$$I_{rel} = \frac{\sum_{\Delta R < 0.3} (E_T + p_T)}{p_T^{\text{lepton}}} \quad (5)$$

where  $p_T$  and  $E_T$  are the transverse momentum and energy of all the particles reconstructed in the  $\Delta R < 0.3$  cone.

Lepton candidates are required to have  $I_{rel} < 0.15$ .

Jet candidates are required to have  $p_T > 40$  GeV and  $\eta < 2.5$ . To avoid leptons to be reconstructed as jets, jet candidates are also required  $\Delta R(\text{jet}, \text{lepton}) > 0.3$ . The medium working point as implemented in Delphes is used in order to identify jets that originate from b quarks.

### 5.1.1. Multiplicities

The lepton, jet and b-tag multiplicity obtained after the before mentioned selection criteria, are shown in figure 3. The top row in figure 3 (a, b, c) corresponds to a 140 PU scenario with a total integrated luminosity of  $3000 \text{ fb}^{-1}$  which is expected in the HL-LHC, while the bottom row (d, e, f) corresponds to a 50 PU scenario with  $L = 300 \text{ fb}^{-1}$ , which is expected during runs II and III. The shapes of the distributions for the 140 PU and 50 PU scenarios are similar, since the event topology does not change. However, the tail of the jet multiplicity distribution in the 140 PU scenario is slightly longer, due to contributions of the PU to the jet energy scale.

The signal events have a high jet and b-jet multiplicity. Moreover, NM1 contains more leptons than NM2 and NM3, and its lepton multiplicity peaks at 1 lepton.

## 5.2. Preselection

In order to select events with a large hadronic activity, events with less than 6 jets ( $p_T^{\text{jet}} > 40$  GeV) are rejected. Events are also required to have at least 4 b-tagged jets, to eliminate contributions from diboson processes, boson + jets and single top.

The distributions of MET and  $H_T$  after the preselection are shown in figure 4 .

## 5.3. Cuts on $H_T$ and MET

Signal events populate on the tails of MET and  $H_T$  distributions. In order to discriminate between background and signal, we reject events that fulfil  $H_T < H_T^{\text{min}}$  and  $\text{MET} < \text{MET}^{\text{min}}$ .  $H_T^{\text{min}}$  and  $\text{MET}^{\text{min}}$  are optimized in order to increase the sensitivity to a new physics signal.

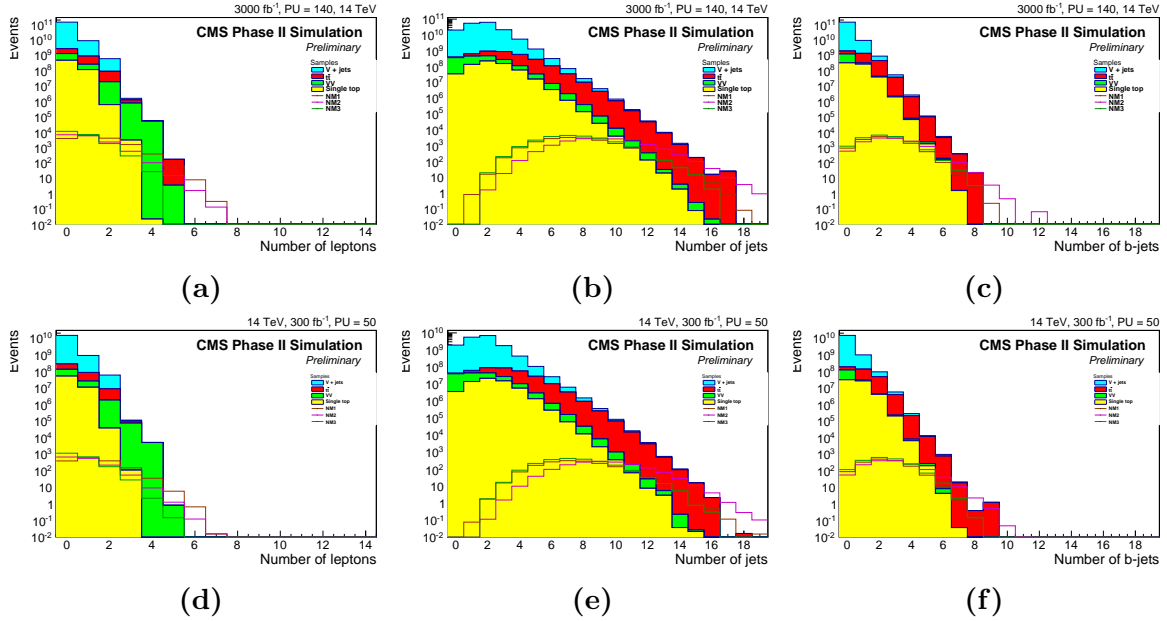


**Figure 3:** Lepton, jet and b-tag multiplicity for  $3000 \text{ fb}^{-1}$  in a 140 PU scenario (a), (b) and (c) and for  $300 \text{ fb}^{-1}$  in a 50 PU scenario (d), (e) and (f).

For that purpose, several figures-of-merit (FOM) can be used. The most common ones are  $S/\sqrt{B}$  and  $S/\sqrt{S+B}$ , but they show bad behaviour in regions of low signal and low background. For that reason, we use an alternative FOM without that kind of behaviour, defined as:

$$T = \frac{\epsilon}{a/2 + \sqrt{B}} \quad (6)$$

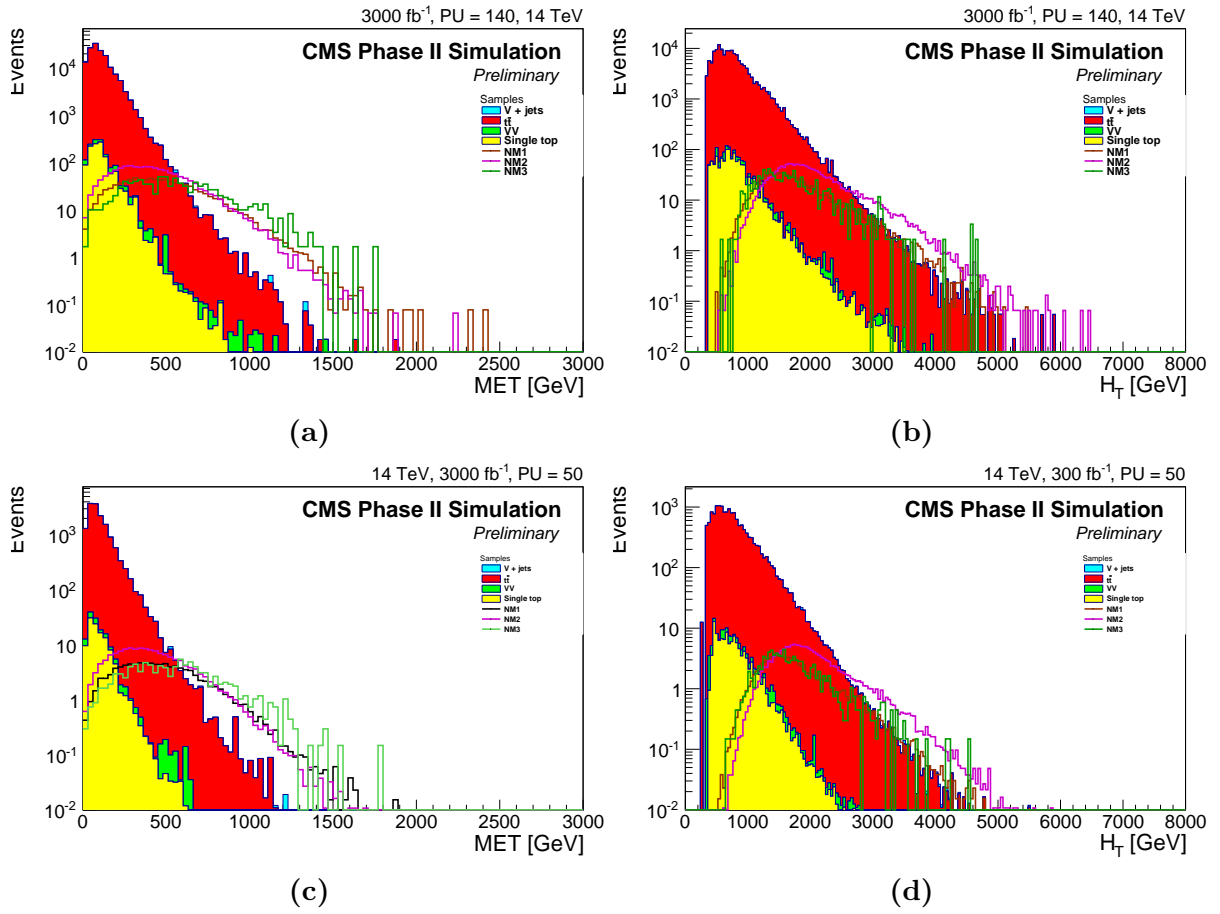
where  $\epsilon$  is the signal efficiency of the analysis ( $\frac{\text{Signal}^{\text{Selected}}}{\text{Signal}^{\text{Generated}}}$ ),  $a$  is the number of sigmas of the analysis and  $B$  is the number of selected background events.

This FOM does not diverge in low background regions and is derived from a statistically sensible definition of sensitivity [13].  $T$  is interpreted as a function of  $H_T^{\text{min}}$  and  $\text{MET}^{\text{min}}$ , which can be optimized. To avoid effects due to correlations, a two-dimensional optimization is performed.

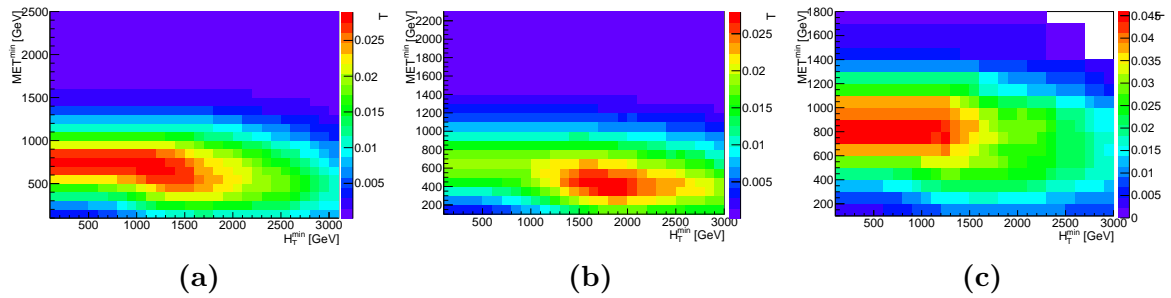
The value of  $T$  for different values of  $(H_T^{\text{min}}, \text{MET}^{\text{min}})$  is plotted in figure 5 for NM1, NM2 and NM3.

Figure 5 shows that the sensitivity dependence on MET is higher than on  $H_T$ . For NM3, the optimal value of  $\text{MET}^{\text{min}}$  is 800 GeV. Given this value of MET, the T function is constant up to 1.3 TeV. A  $H_T^{\text{min}}$  value of 1000 TeV is selected in order to be able to trigger in  $H_T$ . For NM1 and NM3, the T function has a clear peak at  $\text{MET}^{\text{min}} = 600$  GeV and  $H_T^{\text{min}} = 1400$  GeV for NM1 and at  $\text{MET}^{\text{min}} = 400$  GeV and  $H_T^{\text{min}} = 1700$  for NM2.

The optimization does not depend on the luminosity or the pile-up scenario. The optimal selection criteria are also similar when using a looser selection on the number of b-tagged



**Figure 4:** MET and  $H_T$  distribution after the preselection for  $3000 \text{ fb}^{-1}$  in a 140 PU scenario (a), (b) and (c) and for  $300 \text{ fb}^{-1}$  in a 50 PU scenario.



**Figure 5:** T statistic plotted for different values of  $H_T^{\min}$  and  $\text{MET}^{\min}$  for signals NM1 (a), NM2 (b), NM3 (c).

Cut					
SingleLepton	Exactly 1 lepton				
NJets	At least 6 jets				
NBtag	At least 3 b-tagged jets	$H_T/\text{MET}$	400	600	800
METcut (NM1)	MET > 600 GeV	1000			NM3
HTcut (NM1)	$H_T > 1400$ GeV	1400		NM1	
METcut (NM2)	MET > 400 GeV	1700	NM2		
HTcut (NM2)	$H_T > 1700$ GeV				
METcut (NM3)	MET > 800 GeV	(b) Analysis used for every signal. Magnitudes are given in GeV.			
HTcut (NM3)	$H_T > 1000$ GeV				

(a) List of selected cuts.

**Table 3**

jets (at least three b-tags). A list of all selection requirements is summarized in table 3a. The number of selected events for every step and every sample is shown in appendix A. In table 4 the selected events for each sample are summarized.

Sample	Signal	Background
NM1	224	57
NM2	523	121
NM3	201	11

(a) List of selected events for 3000  $fb^{-1}$  and 140 PU scenario.

Sample	Signal	Background
NM1	22	5
NM2	53	13
NM3	19	2

(b) List of selected events for 300  $fb^{-1}$  and 50 PU scenario.

**Table 4**

The  $M_T$  and hard jet multiplicity distributions are shown in figures 7 and 6. Hard jets are those which fulfil the selection criteria and their  $p_T$  is greater than 60 GeV.

## 6. Expected discovery sensitivity

$M_T$  and hard jet multiplicity distributions and the number of signal events selected suggest that it is possible to discover the three models in the HL-LHC. In this section, the expected discovery significance is calculated.

### 6.1. Methods

Two methods are used to calculate the discovery significance.

- BinomObsZ, a function of the package RooStat [14].

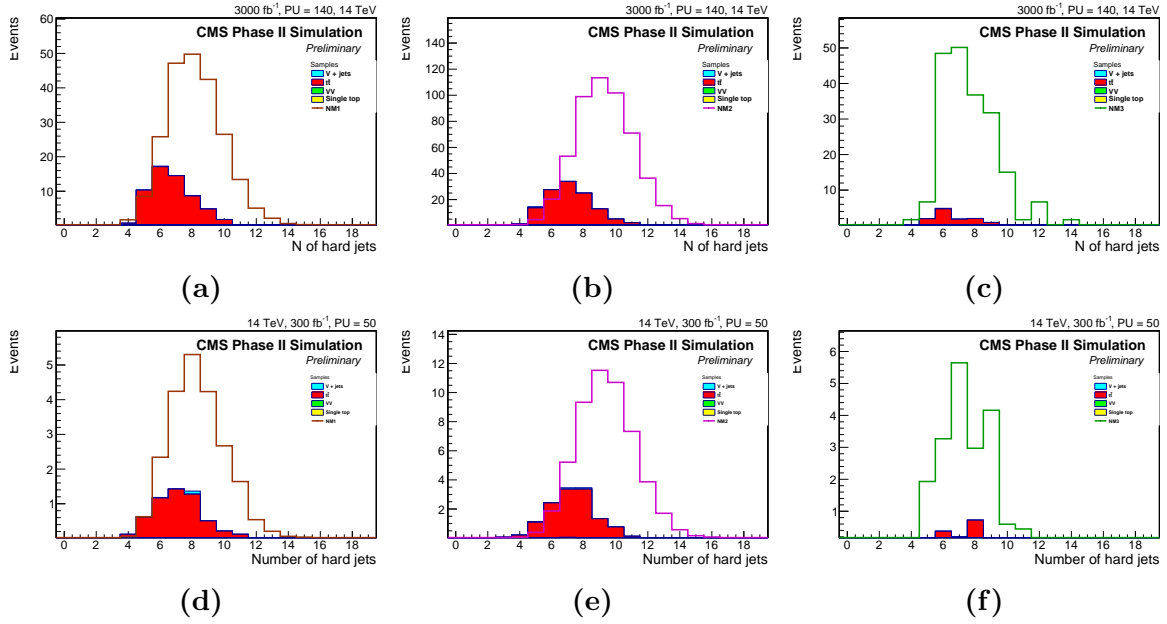


**Figure 6:** Hard jet multiplicity distribution of selected events for NM1 (a), NM2 (b) and NM3 (c) with  $3000 \text{ fb}^{-1}$  and with  $300 \text{ fb}^{-1}$  (d), (e), (f).

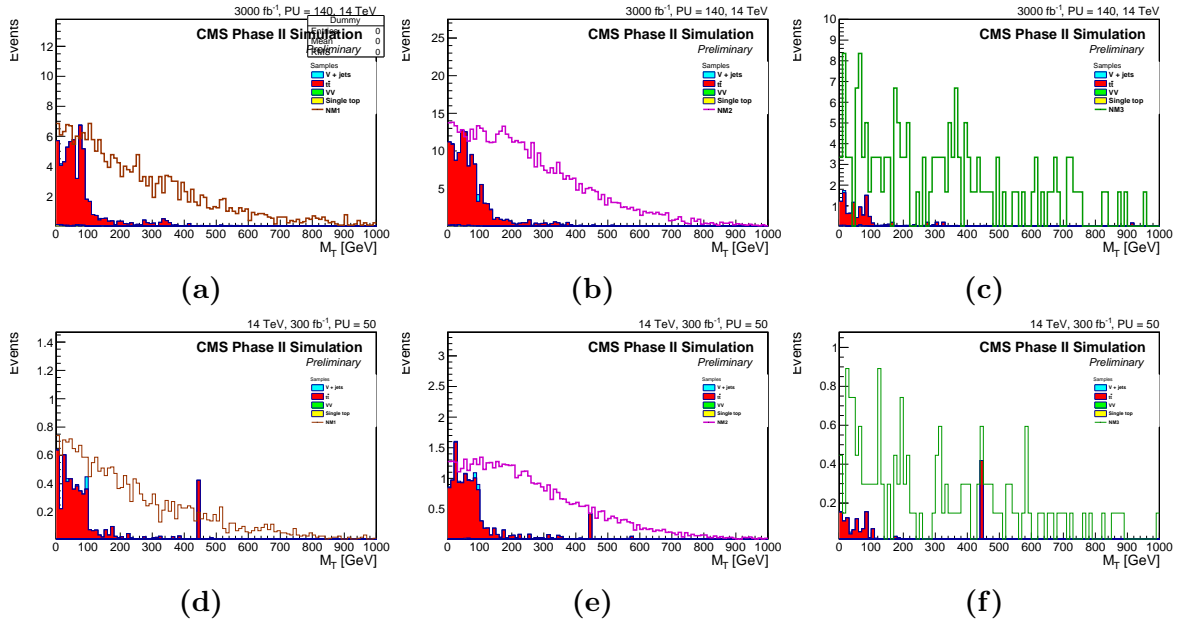


**Figure 7:**  $M_T$  distribution of selected events for NM1 (a), NM2 (b) and NM3 (c) with  $3000 \text{ fb}^{-1}$  and with  $300 \text{ fb}^{-1}$  (d), (e), (f).

- HiggsCombinationTool, in the asymptotical approximation.

The uncertainty of the background is estimated from previous analysis performed with the 8 TeV data [11]. The uncertainty obtained for a similar event selection as shown here is was 50%. This uncertainty is expected to decrease when this analysis can be performed with data, by 2030.

The discovery sensitivities obtained for every model are shown in table 5. The results show that NM3 can be discovered during run III, as the integrated luminosity reaches  $300 \text{ fb}^{-1}$ . The significance rises up to  $7\sigma$  during the HL-LHC.

Discovery will not be possible for NM2 or NM3 even with an integrated luminosity of  $3000 \text{ fb}^{-1}$ . Figure 8a shows the significance versus the total integrated luminosity for a 140 PU scenario. The shape of the graph suggests that the discovery of NM1 and NM3 will not be possible even if the luminosity is increased.

Figure 8b shows the sensitivity as a function of the systematic uncertainty with an integrated luminosity of  $3000 \text{ fb}^{-1}$ . It shows that the  $5\sigma$  necessary to claim discovery can be achieved by decreasing the uncertainty by a 10%.

Sample	BinomObsZ	HiggsCombination tool	Sample	BinomObsZ	HiggsCombination tool
NM1	3.9	3.9	NM1	3.3	3.5
NM2	4.3	4.1	NM2	3.8	3.8
NM3	9.5	7.0	NM3	5.5	5.4

(a)
(b)

**Table 5:** Discovery sensitivity for  $3000 \text{ fb}^{-1}$  (a) and for  $300 \text{ fb}^{-1}$  (b)

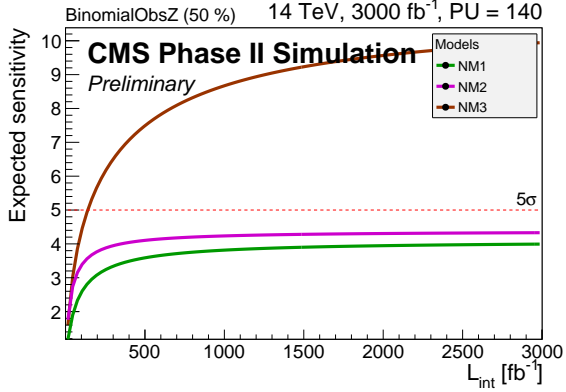
## 6.2. Shape analysis

In order to improve the results obtained, a shape analysis on the number of hard jets is performed. The hard jet distribution is sufficiently different in signal and background to be a good discriminating variable. Moreover, the number of events in each bin is sufficiently high to perform a shape analysis.

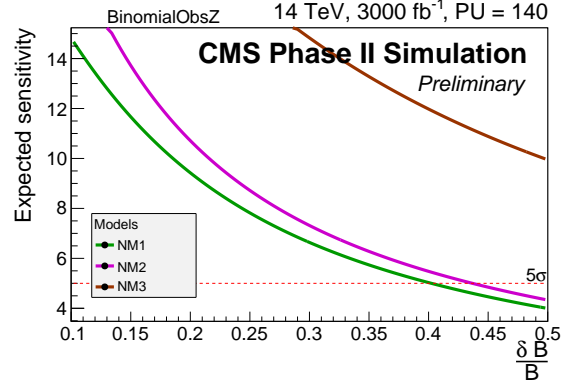
The shape analysis is performed using a binned likelihood, performing a counting analysis on every bin of the distribution.

The range of the histogram is restricted to up to 13 jets for NM1 and NM2 and to up to 11 jets for NM3, in order to avoid empty bins on background.

The results are shown in table 8c. With this method the obtained significances is above 5 sigma with a 50% uncertainty on the overall normalization.



(a) Sensitivity as a function of luminosity for a 140 PU scenario.



(b) Sensitivity as a function of uncertainty for a 140 PU scenario and 3000  $fb^{-1}$ .

Model	Significance
NM1	13.8
NM2	26.5
NM3	12.0

(c) Significances obtained in a shape analysis with the Higgs Combination Tool for 3000  $fb^{-1}$ .

**Figure 8**

## 7. Conclusion

In this study, a SUSY search with one lepton in the final state was performed. The study dealt with the conditions expected during the run of the HL-LHC, including a high pile-up, with an average number of 140 vertices per bunch crossing. These conditions were also compared with another scenario with lower pile-up (50 vertices).

Three SUSY models were taken into account: NM1, NM2, NM3. A study of the decay products of  $\tilde{g}$  in every model revealed that in a large portion of the  $\tilde{g}\tilde{g}$  events a soft lepton is present in the final state. The study of kinematic variables showed a large  $H_T$  and MET, due to presence of top quarks in the SUSY decay cascades and the presence of the LSP in the final state.

These features of the signal model were taken into account to explore the possibility of discovery of these models in pp collisions in LHC. Backgrounds with similar signatures were studied. These signatures included leptons in the final state and large MET.

$H_T$  and MET variables were used in order to discriminate between signal and background. A simple cut and count analysis revealed that NM3 can be discovered with 300  $fb^{-1}$  with a significance of  $5.5\sigma$ . The significance rises to more than  $7\sigma$  for 3000  $fb^{-1}$ . With a simple cut and count analysis, NM1 and NM2 can be observed with 300  $fb^{-1}$  and 3000  $fb^{-1}$ , but the significance will be 3.9 for NM1 and 4.1 for NM2, not enough to claim discovery.

Performing a shape analysis on the hard jet distribution shows a clear discovery for the three models, with a significance higher than  $10\sigma$  in all cases.

In conclusion, the  $3000fb^{-1}$  of data which will be collected during the run of HL-LHC will be necessary to have a proper insight of the SUSY theory, illustrated in this report by the three models NM1, NM2 and NM3.

## **8. Acknowledgments**

I would like to thank all the members of the CMS DESY SUSY group for giving us students an opportunity to participate in their research tasks. I am specially grateful to Claudia Seitz and Isabell Melzer-Pellmann for introducing me to SUSY theory. I would also like make a special mention Batool Safarzadeh and Karim Trippkewitz for their help whenever was needed.

## A. Cut flow

Cut	$t\bar{t}$	V + jets	VV	Single top	Total background	NM1	NM1 ( $\tilde{g}\tilde{g}$ )	$\tilde{g}\tilde{g}$ (%)
NoCuts	$2.16 \cdot 10^9$	$1.69 \cdot 10^{11}$	$1.11 \cdot 10^9$	$6.21 \cdot 10^8$	$1.73 \cdot 10^{11}$	302040	15994	5.3
OneLep	$6.25 \cdot 10^8$	$8.06 \cdot 10^9$	$1.48 \cdot 10^8$	$1.15 \cdot 10^8$	$8.95 \cdot 10^9$	122823	6079	4.9
NJetCut	$1.54 \cdot 10^7$	$3.06 \cdot 10^6$	$2.84 \cdot 10^5$	$1.45 \cdot 10^5$	$1.89 \cdot 10^7$	7662	5266	68.7
BjetCut	146055	1612	219	1187	149073	1029	966	93.9
METCut	104	1	0	1	106	294	282	95.9
HTCut	57	0	0	0	57	224	217	96.9

**Table 6:** Events passing cuts for all backgrounds and NM1 for 3000  $fb^{-1}$  and 140 PU scenario.

Cut	$t\bar{t}$	V + jets	VV	Single top	Total background	NM2	NM2 ( $\tilde{g}\tilde{g}$ )	$\tilde{g}\tilde{g}$ (%)
NoCuts	$2.16 \cdot 10^9$	$1.69 \cdot 10^{11}$	$1.11 \cdot 10^9$	$6.21 \cdot 10^8$	$1.73 \cdot 10^{11}$	213000	15495	100.0
OneLep	$6.25 \cdot 10^8$	$8.06 \cdot 10^9$	$1.48 \cdot 10^8$	$1.15 \cdot 10^8$	$8.95 \cdot 10^9$	59475	5766	51.4
NJetCut	$1.54 \cdot 10^7$	$3.06 \cdot 10^6$	$2.84 \cdot 10^5$	$1.45 \cdot 10^5$	$1.89 \cdot 10^7$	10336	5591	50.7
BjetCut	146055	1612	219	1187	149073	1885	1554	97.1
METCut	1110	21	5	7	1143	875	499	49.5
HTCut	121	1	0	1	123	523	499	45.7

**Table 7:** Events passing cuts for all backgrounds and NM2 for 3000  $fb^{-1}$  and 140 PU scenario.

Cut	$t\bar{t}$	V + jets	VV	Single top	Total background	NM3	NM3 ( $\tilde{g}\tilde{g}$ )	$\tilde{g}\tilde{g}$ (%)
NoCuts	$2.16 \cdot 10^9$	$1.69 \cdot 10^{11}$	$1.11 \cdot 10^9$	$6.21 \cdot 10^8$	$1.73 \cdot 10^{11}$	583000	20470	3.5
OneLep	$6.25 \cdot 10^8$	$8.06 \cdot 10^9$	$1.48 \cdot 10^8$	$1.15 \cdot 10^8$	$8.95 \cdot 10^9$	85077	7067	8.3
NJetCut	$1.54 \cdot 10^7$	$3.06 \cdot 10^6$	$2.84 \cdot 10^5$	$1.45 \cdot 10^5$	$1.89 \cdot 10^7$	7038	5668	80.5
BjetCut	146055	1612	219	1187	149073	1030	974	95.6
METCut	11	0	0	0	11	204	194	95.1
HTCut	11	0	0	0	11	201	192	95.5

**Table 8:** Events passing cuts for all backgrounds and NM3 for 3000  $fb^{-1}$  and 140 PU scenario.

Cut	$t\bar{t}$	V + jets	VV	Single top	Total background	NM1	NM1 ( $\tilde{g}\tilde{g}$ )	$\tilde{g}\tilde{g}$ (%)
NoCuts	$2.16 \cdot 10^8$	$1.69 \cdot 10^{10}$	$1.11 \cdot 10^8$	$6.21 \cdot 10^7$	$1.73 \cdot 10^{10}$	30204	1599	5.3
OneLep	$6.16 \cdot 10^7$	$7.95 \cdot 10^8$	$1.47 \cdot 10^7$	$1.13 \cdot 10^7$	$8.82 \cdot 10^8$	12271	612	5.0
NJetCut	$1.41 \cdot 10^6$	$2.35 \cdot 10^5$	$2.34 \cdot 10^4$	$1.14 \cdot 10^4$	$1.68 \cdot 10^6$	772	533	69.0
BjetCut	14928	51	27	112	15118	105	99	94.3
METCut	10	0	0	0	10	29	28	96.6
HTCut	5	0	0	0	5	22	21	95.5

**Table 9:** Events passing cuts for all backgrounds and NM1 for 300  $fb^{-1}$  and 50 PU scenario.

Cut	$t\bar{t}$	V + jets	VV	Single top	Total background	NM2	NM2 ( $\tilde{g}\tilde{g}$ )	$\tilde{g}\tilde{g}$ (%)
NoCuts	$2.16 \cdot 10^9$	$1.69 \cdot 10^{11}$	$1.11 \cdot 10^9$	$6.21 \cdot 10^8$	$1.73 \cdot 10^{11}$	213000	15495	7.3
OneLep	$6.25 \cdot 10^8$	$8.06 \cdot 10^9$	$1.48 \cdot 10^8$	$1.15 \cdot 10^8$	$8.95 \cdot 10^9$	59475	5766	9.6
NJetCut	$1.54 \cdot 10^7$	$3.06 \cdot 10^6$	$2.84 \cdot 10^5$	$1.45 \cdot 10^5$	$1.89 \cdot 10^7$	10336	5591	54.1
BjetCut	146055	1612	219	1187	149073	1885	1554	82.4
METCut	1110	21	5	7	1143	875	751	85.8
HTCut	121	1	0	1	123	523	499	95.4

**Table 10:** Events passing cuts for all backgrounds and NM2 for 300  $fb^{-1}$  and 50 PU scenario.

Cut	$t\bar{t}$	V + jets	VV	Single top	Total background	NM3	NM3 ( $\tilde{g}\tilde{g}$ )	$\tilde{g}\tilde{g}$ (%)
NoCuts	$2.16 \cdot 10^8$	$1.69 \cdot 10^{10}$	$1.11 \cdot 10^8$	$6.21 \cdot 10^7$	$1.73 \cdot 10^{10}$	588300	2060	0.4
OneLep	$6.16 \cdot 10^7$	$7.95 \cdot 10^8$	$1.47 \cdot 10^7$	$1.13 \cdot 10^7$	$8.82 \cdot 10^8$	8287	699	8.4
NJetCut	$1.41 \cdot 10^6$	$2.35 \cdot 10^5$	$2.34 \cdot 10^4$	$1.14 \cdot 10^4$	$1.68 \cdot 10^6$	694	563	81.1
BjetCut	14928	51	27	112	15118	105	101	96.2
METCut	2	0	0	0	2	19	19	100.0
HTCut	2	0	0	0	2	19	19	100.0

**Table 11:** Events passing cuts for all backgrounds and NM3 for 300  $fb^{-1}$  and 50 PU scenario.

## Acronyms

<b>ALICE</b>	A Large Ion Collider Experiment
<b>ATLAS</b>	A Toroidal LHC Apparatus
<b>CMB</b>	Cosmic Microwave Background
<b>CERN</b>	European Organization for Nuclear Research
<b>cMSSM</b>	Constrained Minimal Supersymmetric Standard Model
<b>CMS</b>	Compact Muon Solenoid
<b>ECAL</b>	Electromagnetic Calorimeter
<b>FOM</b>	Figure-of-merit
<b>GUT</b>	Grand Unified Theory
<b>HL-LHC</b>	High Luminosity LHC
<b>HCAL</b>	Hadronic Calorimeter
<b>LHC</b>	Large Hadron Collider
<b>LHCb</b>	The Large Hadron Collider beauty experiment
<b>LSP</b>	Lightest SUSY Particle
<b>MC</b>	MonteCarlo
<b>MET</b>	Missing Transverse Energy
<b>MSSM</b>	Minimal Supersymmetric Standard Model
<b>NM</b>	Natural Model
<b>PU</b>	Pile-up
<b>SM</b>	Standard Model
<b>SUSY</b>	Supersymmetry
<b>TOE</b>	Theory of Everything

## References

- [1] S. P. Martin, *A Supersymmetry primer*, Adv. Ser. Direct. High Energy Phys. **21** (2010) 1 [hep-ph/9709356].
- [2] I. Melzer-Pellmann, P. Pralavorio *Lessons for SUSY from the LHC after the first run*, *Eur.Phys.J.* **C74** (2014) 2801
- [3] S. Dimopoulos, D. W. Sutter, *The Supersymmetric flavour problem*, *Nucl. Phys.* **B452** (1995) 496-512. doi:10.1016/0550-3213(95)00421-N
- [4] A. Collaboration, *ALICE technical proposal for a large ion collider experiment at the CERN LHC*, *CERN/LHCC* **71** (1995) 1995
- [5] L. Collaboration *et. al.*, *LHCb technical design report, reoptimized detector design and performance*, *CERN/LHCC* **30** (2003)
- [6] G. Aad, *et. al.*, *The ATLAS experiment at the CERN Large Hadron Collider*, *Journal of Instrumentation* **3** (2008) no. 08 808003.
- [7] CMS Collaboration, *The CMS experiment at the CERN LHC*, *JINST* **03** (2008) S08004
- [8] CMS Collaboration, *Identification of b-quark jets with the CMS experiment* *JINST* **8** (2013) P04013
- [9] H. Murayama, *Supersymmetry phenomenology*, hep-ph/0002232.
- [10] CMS Collaboration, *SUSY future analyses for technical proposal*. CMS internal document: SUS-14-012
- [11] CMS Collaboration, "Search for supersymmetry in pp collisions at  $\sqrt{s} = 8$  TeV in events with a single lepton, large jet multiplicity, and multiple b jets", *Phys. Lett. B* 733 (2014) 328.
- [12] J. de Favereau *et al.* [DELPHES 3 Collaboration], *DELPHES 3, A modular framework for fast simulation of a generic collider experiment*, *JHEP* **1402** (2014) 057 [arXiv:1307.6346 [hep-ex]].
- [13] Punzi, *Sensitivity of searches for new signals and its optimization*, arXiv:physics/0308063 [**physics.data-an**]
- [14] Moneta, et al., *The RooStats Project*, arXiv:1009.1003